Pore Size or Geometry: Which Determines the Shape and Inverse-Shape Selective Adsorption of Alkane Isomers?

Jianwen Jiang*

Department of Chemical & Biomolecular Engineering, National University of Singapore, 4 Engineering Drive 4, Singapore 117576, Singapore

Received: January 11, 2006; In Final Form: March 18, 2006

The adsorption of pure pentane (C_5) isomers and their ternary mixture is simulated in a series of carbon nanoslits. With decreasing nanoslit pore size, shape selective adsorption first occurs in the order of n-$C_5 \geq i$-$C_5 > neo$-C_5 due to the configurational entropy effect, then inverse-shape selective adsorption occurs in the order of n-$C_5 < i$-$C_5 \leq neo$-C_5 due to the area entropy effect, and finally no adsorption occurs. The entropy effects lead to a large adsorptive separation among the C_5 isomers from their mixture. Similar behavior has been observed from the simulation of C_5 adsorption in carbon nanotubes with variation in pore size. These results reveal that pore size rather than geometry determines the shape and inverse-shape selective adsorption of alkane isomers in nanopores.

I. Introduction

Alkane (C_n) isomers can be separated by selective adsorption on the basis of the differences in their molecular shape.[1] With a proper choice of substrate, C_n isomers can exhibit intriguing shape or inverse-shape selective adsorption. Santilli[2] first proposed the concept of shape selectivity from the adsorption of C_6 isomer mixtures in zeolites, in which the adsorption capacity was found to decrease with increased degree of branching. Denayer et al.[3] measured the limiting adsorption properties and separation factors of C_5-C_8 isomers in zeolites, and found shape selective adsorption among the isomers depending on zeolite type. Calero et al.[4] and Krishna et al.[5,6] simulated the isotherms of C_5-C_7 isomers in MFI silicalite, and observed the following adsorption order linear > monobranched > dibranched as a result of the configurational entropy effect. Schenk et al.[7] computed the contribution of zeolites to the free energies of formation for alkane isomers, and revealed that shape selectivity plays an important role in alkane cracking/conversion within zeolites.

Inverse-shape selective adsorption has also been observed from experimental and simulation studies. Santilli et al.[8] found the preferential adsorption of 2,2-dimethyl-C_4 and 3-methyl-C_5 over n-C_6 in SAPO-5 and MOR zeolites. Denayer et al.[9] reported both shape and inverse-shape selective adsorption of C_4-C_8 isomers at the Henry regime in SAPO-5, and interpreted the occurrence of shape versus inverse-shape selectivity in terms of a counterbalance between adsorption enthalpy and entropy. Krishna et al.[5,6] simulated the adsorption of C_6 isomers in AFI and MOR, and the extent of adsorption at high coverages was found to be linear < monobranched < dibranched as a result of the length entropy effect. Schenk et al.[10,11] demonstrated from simulation that inverse-shape selectivity may be important in the zeolite catalysis of alkane reactions. Fox and Bates[12] simulated the adsorption of binary and ternary mixtures of linear, branched, and cyclic C_6 isomers in silicalite, $AlPO_4$-5, and ITQ-22, and found shape selectivity at 300 K, but inverse-shape selectivity at 600 K. This temperature-dependent adsorption selectivity was regarded to be a consequence of the isomer shape change with temperature. Denayer et al.[13] observed preferential adsorption of C_3-C_7 isoalkanes over their linear isomers in zeolite cages driven by rotational entropy.

The adsorption of C_5 isomers was recently investigated by using molecular simulation in a series of open-ended armchair-type single-walled carbon nanotubes (SWNTs).[14] The shape selective adsorption occurs only in a (7,7) SWNT, while the inverse-shape selective adsorption occurs in larger SWNTs. The pore size of SWNT was found to be crucial as to which type of selective adsorption occurs.

An intriguing question is whether the shape and inverse-shape selective adsorption can be observed in other types of nanopores, e.g., nanoslit? The pore geometry of nanoslit is different from that of SWNT. Between pore size and geometry, which determines the occurrence of shape and inverse-shape selectivity? This is addressed in the current work by simulating the adsorption of pure and mixed C_5 isomers in a series of nanoslits.

II. Model and Method

Two models are usually used to mimic an alkane molecule, the united-atom model and the all-atom model.[15] Both models were found to yield comparable adsorption isotherms for alkane adsorption in silicalite; nevertheless, the computation was faster by using the simpler united-atom model.[16] Consequently, as in our previous studies,[14,17,18] the united-atom model was used here, in which each CH_x group was represented as a single interaction site. The C−C bonds were assumed to be rigid and fixed at 1.53 Å. The alkane−alkane interactions included bond bending, dihedral torsion, and nonbonded Lennard-Jones dispersion. The force field parameters used were those reported by Martin and Siepmann[19,20] to accurately reproduce experimental vapor−liquid coexistence curves and critical properties of pure linear and branched alkanes. The LJ parameters of unlike alkane sites were obtained by using the Jorgensen combining rules[21] $\epsilon_{ij} = \sqrt{\epsilon_i \epsilon_j}$ and $\sigma_{ij} = \sqrt{\sigma_i \sigma_j}$. A cutoff length of 20 Å was used in the calculation of the LJ interaction energies, and no long-range correction was added.

* Address correspondence to the author at e-mail chejj@nus.edu.sg, phone (65) 6516 5083, or fax (65) 6779 1936.

10.1021/jp060213w CCC: $33.50
Published on Web 04/12/2006

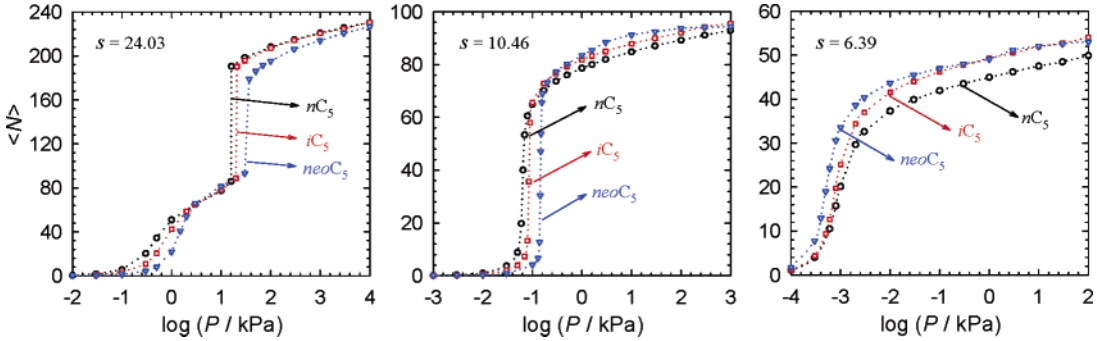

Figure 1. Adsorption isotherms for pure C_5 isomers in nanoslits with pore size $s = 24.03$, 10.46, and 6.39 Å. The lines are drawn for visual clarity.

The carbon nanoslit was modeled as two graphitic basal surfaces separated by a width w in the z dimension. The width w is the center-to-center distance between carbon atoms at the edge of each surface, the accessible "pore size" s is thus approximated by $s = w - 3.1$, in which 3.1 Å is the van der Waals diameter of the carbon atom.[22] The length of the slit surface in the x or y dimension was assumed to be 40 Å. The periodic boundary conditions were employed in the transverse xy plane parallel to the slit surface. The nonbonded dispersion between a slit surface and an alkane site was modeled by Steele's 10-4 potential[23]

$$u_{sa}(z) = 2\pi\rho_s\epsilon_{sa}\sigma_{sa}^2\Delta\sum_{l=0}^{\infty}\left[\frac{2}{5}\left(\frac{\sigma_{sa}}{z+l\Delta}\right)^{10} - \left(\frac{\sigma_{sa}}{z+l\Delta}\right)^{4}\right] \quad (1)$$

where z is the distance from the uppermost plane of the slit surface, $\rho_s = 0.114$ (Å)$^{-3}$ is the implicit carbon number density of the slit surface, ϵ_{sa} is the cross well depth estimated from the Jorgensen combing rule[21] with $\epsilon_{ss}/k_B = 28.0$ K, σ_{sa} is the cross collision diameter set to 3.60 Å for each alkane site, and $\Delta = 3.35$ Å is the distance of graphene sheets. Equation 1 can be accurately approximated by Steele's 10-4-3 potential[23]

$$u_{sa}(z) = 2\pi\rho_s\epsilon_{sa}\sigma_{sa}^2\Delta\left[\frac{2}{5}\left(\frac{\sigma_{sa}}{z}\right)^{10} - \left(\frac{\sigma_{sa}}{z}\right)^{4} - \left(\frac{\sigma_{sa}^4}{3\Delta(0.61\Delta+z)^3}\right)\right] \quad (2)$$

Overall, the interaction potential of an alkane site in the slit pore is $u_{sa}(z) + u_{sa}(w - z)$.

Grand canonical Monte Carlo (GCMC) simulations[24,25] were carried out to predict the adsorption isotherms of pure C_5 isomers and their ternary mixture in carbon nanoslits at room temperature $T = 300$ K. For the conditions in this study, the reservoir was assumed to behave as an ideal gas. To improve the efficiency of sampling alkane molecules, the advanced configurational-bias method was employed.[25] Rather than inserting a molecule at a random position as in conventional techniques, in the configurational-bias method a molecule is grown atom-by-atom biasing energetically favorable configurations while avoiding overlap with other atoms, and the bias is then removed by adjusting the acceptance rules. A typical GCMC simulation was performed for a total 20 000 cycles, in which the first 10 000 cycles were used for equilibration, and the second 10 000 cycles were used to sample ensemble averages. The block transformation method was used to estimate the statistical uncertainties of the simulated averages.[25] Unless otherwise stated, the uncertainties are smaller than the symbol size in the figures presented in the next section. Each cycle consisted of a number of the following attempted trial moves: translation, rotation, partial regrowth, complete regrowth, exchange with the reservoir, and exchange of molecular identity (only for a mixture). The acceptance rules for these trial moves can be found elsewhere.[25] For the adsorption of a pure alkane, each cycle consisted of 5 000 trial moves with the following relative probabilities: 10% translation, 10% rotation, 10% partial regrowth, 10% complete regrowth, and 60% exchange with the reservoir. For the adsorption of a mixture, the number of trial moves in each cycle was increased to 20 000 to ensure mechanical and compositional equilibrium; the relative probability for exchange with the reservoir was decreased to 55%, and a 5% probability was assigned for the exchange of molecular identity. Within the statistical uncertainty, the simulation results were independent of the choice of the trial moves.

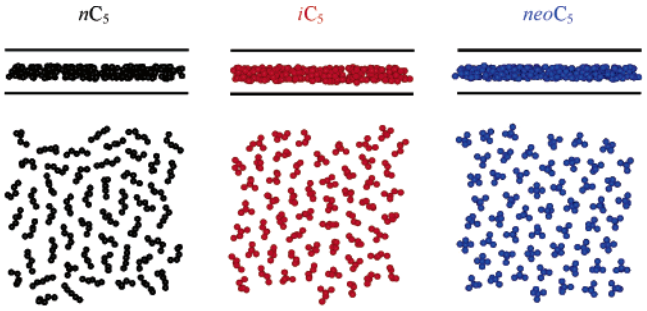

Figure 2. Equilibrium snapshots for pure C_5 isomers in nanoslit with pore size $s = 6.39$ Å at 100 kPa. The tops are views in the (100) or the (010) plane, and the bottom is in the (001) plane.

III. Results

The adsorption isotherms for pure C_5 isomers in a series of nanoslits were simulated. Figure 1 shows three typical isotherms in nanoslits with accessible pore size $s = 24.03$, 10.46, and 6.39 Å. Here $\langle N\rangle$ is the ensemble averaged total number of C_5 molecules in a nanoslit with a volume of $40 \times 40 \times w$ (Å)^3. As seen in a (20,20) SWNT with $s = 24.03$ Å,[14] C_5 adsorption in a nanoslit with identical pore size also exhibits shape selectivity in the order of $nC_5 \geq iC_5 > neoC_5$. The difference from that in a (20,20) SWNT is capillary condensation occurs here at the onset pressures of about 16, 20, and 33 kPa for nC_5, iC_5, and $neoC_5$. This implies that the capillary critical temperature is lower than 300 K in a (20,20) SWNT, while higher than 300 K in a nanoslit with the same pore size. This is in accord with our recent work, in which the confinement effect was found to be stronger in a cylindrical nanotube than in a nanoslit of the same size.[26] The observed shape selectivity is due to the configurational entropy effect. With increased degree of branching, the C_5 isomer changes from slender to bulky. Steric hindrance prevents a bulky molecule from adopting a close-packed adsorption configuration; consequently, a linear isomer is preferentially adsorbed over a branched isomer. Similar

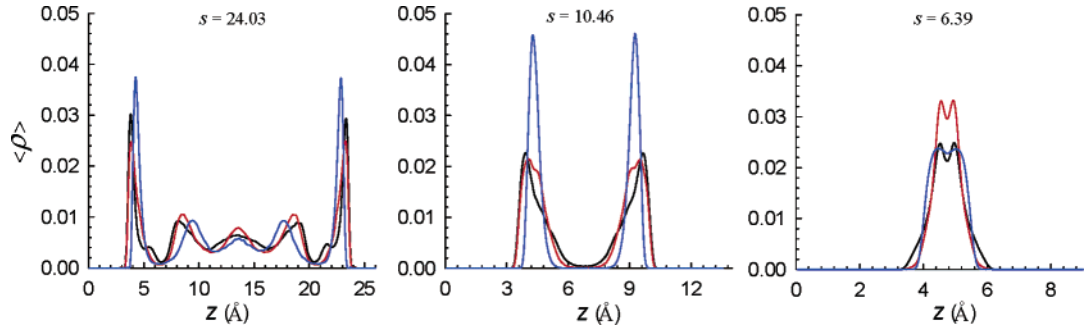

Figure 3. Density profiles for the center-of-mass of pure C_5 isomers in nanoslits with pore size $s = 24.03$, 10.46, and 6.39 Å at 100 kPa. The lines are drawn for visual clarity.

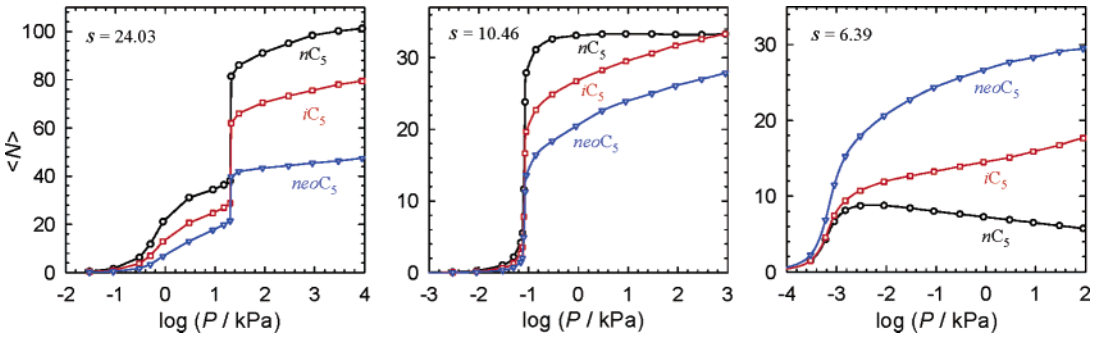

Figure 4. Adsorption isotherms for an equimolar mixture of C_5 isomers in nanoslits with pore size $s = 24.03$, 10.46, and 6.39 Å. The lines are drawn for visual clarity.

shape selective behavior has been observed in the adsorption of alkane isomers in zeolites of intermediate and large channel size.[2−6] In a nanoslit with $s = 10.46$ Å, the adsorption is shape selective at low pressures, but changes to inverse-shape selective at high pressures. In a (10,10) SWNT with $s = 10.46$ Å, however, shape selective adsorption was observed over a wide range of pressure.[14] In a nanoslit with $s = 6.39$ Å, the adsorption order is *neo*$C_5 \geq i$$C_5 > n$$C_5$, similar to the adsorption in a (7,7) SWNT with identical pore size.[14] Opposite to the shape selectivity in larger nanoslits, this inverse-shape selectivity is related to the area entropy effect. Our results are consistent with previous studies, in which the inverse-shape selectivity was reported in SAPO-5, MOR, and AFI zeolites with channels of approximately 6.5−7.5 Å.[5,6,8−11] In a nanoslit with $s = 5.0$ Å, $n$$C_5$ and $i$$C_5$ can enter the pore easily, but *neo*C_5 is detected only at high pressures. In this situation, the nanoslit may act as a molecular sieve allowing some isomers to enter the pore while the others are blocked, as is the case for small-pore zeolites SSZ-16,[2] erionite,[2] and 5A.[27] In a nanoslit with $s = 4$ Å, *neo*C_5 cannot enter the pore even at high pressures. In a still smaller nanoslit, e.g., with $s = 3$ Å, none of the C_5 isomers can enter the pore.

Figure 2 shows typical simulation snapshots of pure C_5 isomers at equilibrium adsorbed in a nanoslit with $s = 6.39$ Å at 100 kPa, in which the adsorption of each isomer is close to saturation. The nanoslit is sufficiently wide in the z dimension for C_5 molecules to enter the pore, but only allows them to be arranged in one transverse xy layer preferentially near the nanoslit center. With increased degree of branching in the C_5 isomer, the molecular cross section area becomes larger, whereas the transverse area becomes smaller. The inverse-shape selective adsorption occurring in the nanoslit is a consequence of the transverse area entropy effect. A C_5 isomer with a less transverse area can pack most compact within the planar adsorption layer. This behavior is similar to the inverse-shape adsorption in (7,7) SWNT due to the length entropy effect.

Figure 3 shows the density profiles for the center-of-mass of pure C_5 isomers as a function of the distance z from a nanoslit surface at 100 kPa in three nanoslits with $s = 24.03$, 10.46, and 6.39 Å. As the two nanoslit surfaces are identical, the density profiles are symmetrical at $z = w/2$. In a nanoslit with $s = 24.03$ Å, for each isomer there are five adsorption layers sequentially from one surface to the other. The most favorable adsorption sites are close to the surfaces, therefore, the density profiles have the largest peaks near surfaces. Away from the surfaces, the peaks are lower because of a weaker attraction. In a nanoslit with $s = 10.46$ Å, there are two symmetrical peaks for each isomer, and no peak at the nanoslit center. In a nanoslit with $s = 6.39$ Å, as seen from the snapshots in Figure 2, each C_5 isomer adsorbs around the nanoslit center, and a peak is thus observed only near the center.

Figure 4 shows the adsorption isotherms for an equimolar mixture of three C_5 isomers in three nanoslits with $s = 24.03$, 10.46, and 6.39 Å. As seen in Figure 1, the differences between the adsorption extents of the pure isomers are generally small. By contrast, the differences are substantially large among isomers from the adsorption of mixture in all three nanoslits. In a nanoslit with $s = 24.03$ Å, the configurational entropy effect enhances the shape selectivity, and the adsorption extent is $n$$C_5 > i$$C_5 >$ *neo*C_5. Intriguingly, capillary condensation occurs here at a nearly identical onset pressure of about 20 kPa for all three isomers, rather than at three different onset pressures as seen in Figure 1 for pure isomers. This is because the formation of the liquid phase of one isomer facilitates other isomers to condense. In a first-order phase transition, initially the nucleus starts to form and aggregate. When the nucleus reaches a critical size, a new phase appears and grows spontaneously. The existing critical nucleus and new phase of a substance can facilitate the instantaneous formation of a new phase for other substances. Although the three isomers condense at the same onset pressure, they interact differently with the nanoslit leading to different adsorption capacities. In a nanoslit with $s = 10.46$ Å, adsorption

is shape selective at high pressures, different from the adsorption of pure isomers. In a nanoslit with $s = 6.39$ Å, the inverse-shape selective adsorption occurs in the order of *neo*C_5 > *i*C_5 > *n*C_5.

IV. Conclusions

In current work, simulation results for the shape and inverse-shape selective adsorption of C_5 isomers in carbon nanoslits are presented. The pore size of the nanoslit is found to be crucial as to which type of selective adsorption dominates. The shape selective adsorption occurs in larger nanoslits due to the configurational entropy effect, while the inverse-shape selective adsorption occurs due to the transverse area entropy effect. The entropy effects are enhanced in the adsorption of a mixture of isomers, and lead to larger adsorption selectivity. Similar results have been obtained in the adsorption of C_5 isomers in carbon nanotubes as a function of pore size. The work reveals that the subtle balance of entropy effect is essential in determining the adsorption behavior of alkane isomers in nanopores, and pore size rather than geometry determines the occurrence of the shape and inverse-shape selective adsorption. Finally, this work suggests that carbon nanotubes or nanoslits may be utilized in the development of a novel process for the separation of alkane isomers.

Acknowledgment. The author is grateful for the support from the National University of Singapore.

References and Notes

(1) Chen, N. Y.; Garwood, W. E.; Dwyer, F. G. *Shape Selective Catalysis in Industrial Applications*; Marcel Dekker: New York, 1989.
(2) Santilli, D. S. *J. Catal.* **1986**, *99*, 335.
(3) Denayer, J. F.; Souverijns, W.; Jacobs, P. A.; Martens, J. A.; Baron, G. V. *J. Phys. Chem. B* **1998**, *102*, 4588.
(4) Calero, S.; Smit, B.; Krishna, R. *Phys. Chem. Chem. Phys.* **2001**, *3*, 4390.
(5) Krishna, R.; Smit, B.; Calero, S. *Chem. Soc. Rev.* **2002**, *31*, 185.
(6) Smit, B.; Krishna, R. *Chem. Eng. Sci.* **2003**, *58*, 557.
(7) Schenk, M.; Smit, B.; Vlugt, T. J. H.; Maesen, T. L. M. *Angew. Chem., Int. Ed.* **2001**, *40*, 736.
(8) Santilli, D. S.; Harris, T. V.; Zones, S. I. *Microporous Mater.* **1993**, *1*, 329.
(9) Denayer, J. F. M.; Ocakoglu, A. R.; Martens, J. A.; Baron, G. V. *J. Catal.* **2004**, *226*, 240.
(10) Schenk, M.; Calero, S.; Maesen, T. L. M.; van Benthem, L. L.; Verbeek, M. G.; Smit, B. *Angew. Chem., Int. Ed.* **2002**, *41*, 2500.
(11) Schenk, M.; Calero, S.; Maesen, T. L. M.; Vlugt, T. J. H.; van Benthem, L. L.; Verbeek, M. G.; Schnell, B.; Smit, B. *J. Catal.* **2003**, *214*, 88.
(12) Fox, J. P.; Bates, S. P. *J. Phys. Chem. B* **2004**, *108*, 17136.
(13) Denayer, J. F. M.; Ocakoglu, A. R.; Arik, I. C.; Krischhock, C. E. A.; Martens, J. A.; Baron, G. V. *Angew. Chem., Int. Ed.* **2005**, *44*, 400.
(14) Jiang, J. W.; Sandler, S. I. *J. Chem. Phys.* **2006**, *124*, 024717.
(15) Ryckaert, J. P.; Bellemans, A. *Faraday Discuss. Chem. Soc.* **1978**, *66*, 95.
(16) Macedonia, M. D.; Maginn, E. J. *Fluid Phase Equilib.* **1999**, *158*−*160*, 19.
(17) Jiang, J. W.; Sandler, S. I.; Schenk, M.; Smit, B. *Phys. Rev. B* **2005**, *72*, 045447.
(18) Jiang, J. W.; Sandler, S. I.; Smit, B. *Nano Lett.* **2004**, *4*, 241.
(19) Martin, M. G.; Siepmann, J. I. *J. Phys. Chem. B* **1998**, *102*, 2569.
(20) Martin, M. G.; Siepmann, J. I. *J. Phys. Chem. B* **1999**, *103*, 4508.
(21) Jorgensen, W. L.; Madura, J. D.; Swenson, C. J. *J. Am. Chem. Soc.* **1984**, *106*, 6638.
(22) We have used the default value of 3.1 in V*iewerLite 4.2* (Accelrys Inc). The value of 3.0 was used in: Corey, R. B.; Pauling, L. *Rev. Sci. Instrum.* **1952**, *24*, 621. The value of 3.4 was used in: Fujiwara, A.; et al. *Chem. Phys. Lett.* **2001**, *336*, 205. Kukovecz, A.; et al. *Phys. Chem. Chem. Phys.* **2003**, *5*, 582; Kis, A.; et al. *Nature Mater.* **2004**, *3*, 153.
(23) Steele, W. A. *The Interaction of Gases with Solid Surfaces*; Pergamon: Oxford, UK, 1974.
(24) Allen, M. P.; Tildesley, D. J. *Computer simulation of liquids*; Clarendon Press: Oxford, UK, 1987.
(25) Frenkel, D.; Smit, B. *Understanding Molecular Simulations*: *From algorithms to applications*, 2nd ed.; Academic Press: San Diego, CA, 2002.
(26) Jiang, J. W.; Sandler, S. I. Submitted for publication, 2006.
(27) Broughton, D. B. *Chem. Eng. Prog.* **1968**, *64*, 60.